Available online at www.sciencedirect.com
ScienceDirect
Tetrahedron
Tetrahedron 63 (2007) 148–154

# Gloriosaols A and B, two novel phenolics from *Yucca gloriosa*: structural characterization and configurational assignment by a combined NMR-quantum mechanical strategy

Carla Bassarello,[a] Giuseppe Bifulco,[a,*] Paola Montoro,[a] Alexandre Skhirtladze,[b] Ether Kemertelidze,[b] Cosimo Pizza[a] and Sonia Piacente[a,*]

[a]*Dipartimento di Scienze Farmaceutiche, Università degli Studi di Salerno, Via Ponte Don Melillo, 84084 Fisciano, Salerno, Italy*
[b]*Institute of Pharmacochemistry, Tbilisi, Georgia*

Received 26 July 2006; revised 19 September 2006; accepted 12 October 2006
Available online 2 November 2006

**Abstract**—Gloriosaols A (**1**) and B (**2**), two novel phenolic derivatives characterized by unusual spirostructures made up of two $C_{15}$ units linked via a γ-lactone to a central stilbenic portion were isolated from the roots of *Yucca gloriosa*. On the basis of an extensive NMR analysis, the same basic structure was established for the two compounds but no further information about their structural difference could be deduced. Thus two hypotheses were formulated: (1) gloriosaols A and B could be atropisomers caused by a restriction of the free rotation around the double bond due to a steric congestion of the bulky phenolic portions; (2) gloriosaols A and B could be two configurational isomers, indicating, in this case, a nonstereoselective biogenetic formation of the stereogenic center C-2. Semi-empirical calculations of the potential energy surfaces on gloriosaols A and B, together with the $^1$H NMR spectra recorded at various temperatures, allowed us to unambiguously exclude the hypothesis of two restricted rotational conformers of a single configurational isomer. Finally, quantum mechanical calculations of the geometries and of the $^1$H chemical shifts on the gloriasols A and B in combination with the analysis of the ROE data allowed us to deduce a diastereomeric relation between the two compounds and to assess the relative configuration of the two diastereomers.


## 1. Introduction

Continuing our studies on *Yucca* spp., we have undertaken the investigation of the phenolic fraction of the roots of *Yucca gloriosa* (Agavaceae), a species largely cultivated in Eastern Georgia where industrial plantations occupy a total area of about 150 hectares. This plant is a rich source of steroidal saponins and the saponin fraction of its leaves has been used as raw material for the synthesis of 5α steroid hormones.[1] Investigations carried out until now have been focused only on the characterization of the saponin constituents.[2–4]

Our previous investigation of the bark of the better known *Yucca schidigera* (*Yucca*) resulted in the isolation of the stilbenic derivatives resveratrol, *trans*-3,3′,5,5′-tetrahydroxy-4′-methoxystilbene, the spirobiflavonoid larixinol along with novel phenolic derivatives with very unusual spirostructures, named yuccaols A–E and yuccaone A.[5–8]

Resveratrol is the natural phytoalexin found in considerable amounts in the skin of grapes,[9,10] mulberries, and peanuts,[11] and in some medicinal plants.[12,13] In the last 15 years this compound has received a lot of attention because of its anti-oxidant,[14] anti-inflammatory,[15] and anti-carcinogenic[16–18] properties. The multifunctional activities of resveratrol together with the novelty of yuccaols A–E, structurally related to resveratrol,[8] prompted us and our coauthors to carry out a program aimed to evaluate for yucca phenolics some of the activities exerted by resveratrol.[7,8,19–22] In this context, a strong radical scavenging activity was observed for all yucca phenolics.[7] Furthermore, the evaluation of the inhibitory effects of yucca phenolics on thrombin-induced platelet aggregation revealed that these compounds showed even stronger anti-platelet activity than resveratrol.[19] They also had an inhibitory effect on the thrombin-induced enzymic platelet lipid peroxidation and inhibited the generation of free radicals in blood platelets activated by thrombin or thrombin receptor activating peptide (TRAP). Comparative studies using in vitro tests showed that all the phenolics from yucca bark exerted an antioxidant effect on different ROS produced in resting blood platelets and blood platelets activated by thrombin or TRAP.[20] Furthermore, yuccaol C was found to inhibit significantly, in a dose related manner, nitrogen oxide generation

*Keywords*: *Yucca gloriosa*; Resveratrol; Gloriosaols A and B; GIAO NMR; DFT calculations.
* Corresponding authors. Tel.: +39 089 969741; fax: +39 089 969602 (G.B.); tel.: +39 089 969763; fax: +39 089 969602 (S.P.); e-mail addresses: bifulco@unisa.it; piacente@unisa.it

0040–4020/$ - see front matter © 2006 Published by Elsevier Ltd.
doi:10.1016/j.tet.2006.10.034

in activated macrophages and to reduce the expression of the inducible isoform of nitrogen oxide synthase (iNOS).[21] NO produced by iNOS is a key mediator in inflammatory processes and its production is a crucial step in both the immunoresponsive cells. In a recent study,[22] yuccaols A–C were found to inhibit in a dose-dependent manner the vascular endothelial growth factor (VEGF)-induced proliferation, migration, and PAF biosynthesis in Kaposi's sarcoma (KS) cells. PAF is a potent mediator of inflammation, it is known to promote angiogenesis and in vitro migration of endothelial cells and KS cells. Thus, these results suggest that the anti-inflammatory properties attributed to *Y. schidigera* can be ascribed to resveratrol and yuccaols A–C and provide the first evidence for the anti-cancer and anti-invasive properties of yuccaols.

On this basis, we deemed it of interest to investigate the phenolic fraction of *Y. gloriosa*. This study led to the isolation of two new phenolic constituents namely gloriosaols A and B. They resulted to be made up of two $C_{15}$ units probably derived from a flavonoid skeleton linked via a γ-lactone ring to a central stilbenic moiety corresponding to *trans*-3,3′,5,5′-tetrahydroxy-4′-methoxystilbene. The structures of these compounds were elucidated by extensive spectroscopic methods including 1D ($^1$H and $^{13}$C) and 2D NMR experiments (DQF-COSY, HSQC, HMBC, and ROESY) as well as HR-ESI-MS analysis. The close similarity between the two compounds, which differed only in the configuration of two stereogenic carbons, prompted us to apply a strategy based on the quantum mechanical calculation of the NMR properties of the two possible stereoisomers, and their comparison with experimental data.[23] On this basis, it was possible to assign the relative configuration of the two compounds.

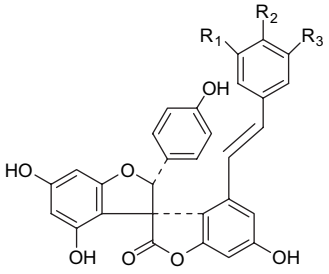


yuccaol A $R_1$ = H $R_2$ = OH $R_3$ = H
yuccaol D $R_1$ = OH $R_2$ = OMe $R_3$ = OH

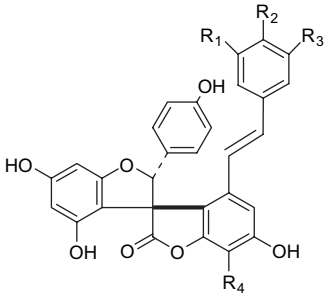


yuccaol B $R_1$ = H $R_2$ = OH $R_3$ = H $R_4$ = H
yuccaol C $R_1$ = OH $R_2$ = OMe $R_3$ = OH $R_4$ = H
yuccaol E $R_1$ =OH $R_2$ = H $R_3$ = OH $R_4$ = OMe

## 2. Results and discussion

### 2.1. Determination of the basic structure of gloriosaols A and B

The phenolic portion of *Y. gloriosa* bark subjected to Sephadex LH-20 and then to RP-HPLC using $CH_3CN$–$H_2O$ (35:65) as eluent afforded two new phenolic derivatives, namely gloriosaols A and B.

The ESI-MS spectra in the positive ion mode of the two compounds showed a protonated molecular ion $[M+H]^+$ at *m/z* 811 and a sodium-containing molecular ion $[M+Na]^+$ at *m/z* 833 corresponding to the molecular formulae $C_{45}H_{31}O_{15}$ and $C_{45}H_{30}O_{15}Na$, respectively. ESI-MS/MS spectra of the peak at *m/z* 811 gave a product ion spectrum characterized by an intense peak at *m/z* 269, corresponding to a protonated stilbene unit and minor peaks at *m/z* 717 and 419.

The $^1$H NMR spectrum of gloriosaol A (Table 1) showed four doublets at δ 6.71, 6.73, 6.90, and 6.91 (2H each, d, *J*=8.5 Hz) typical of *ortho*-coupled aromatic protons along with signals ascribable to a trans-disubstituted double bond at δ 7.06 and 7.00 (1H each, d, *J*=16.1 Hz), to three pairs of *meta*-coupled protons at δ 5.96, 5.98, 6.16, 6.17, 6.41, and 6.47 (1H each, d, *J*=1.8 Hz), to three uncoupled protons at δ 5.83, 5.86, 6.57, and to a methoxy group at δ 3.84. The COSY experiment showed the couplings between the signals at δ 6.71 and 6.91, 6.73 and 6.90, 5.96 and 6.16, 5.98 and 6.17, 6.41 and 6.47. In the $^{13}$C NMR spectrum (Table 1), except for the signals at δ 60.9, 62.1, and 62.3, all the carbon signals appeared in the lower magnetic field region (δ>90 ppm). The protonated carbons (20) and their corresponding protons were unambiguously assigned by the HSQC experiment. The quaternary carbons (25) were sorted into 23 $sp^2$ carbons, among which 15 resulted to be oxygenated, and 2 $sp^3$ carbons. These spectroscopic data implied a highly oxygenated and highly unsaturated structure for gloriosaol A. The HMBC correlations clearly showed that gloriosaol A was made up of two identical $C_{15}$ fragments linked to a central stilbenic moiety. In particular the long-range correlations between the proton signal at δ 6.57 and the carbon resonances at δ 119.5, 125.9, 130.2, 133.5, 151.7; the proton signal at δ 6.47 and the carbon resonances at δ 98.5, 118.2, 126.8, 137.0, 160.3; the proton signal at δ 6.41 and the carbon resonances at δ 108.3, 118.2, 155.6, 160.3 allowed us to identify the stilbenic core as a 2,2′-di-*C*-substituted *trans*-3,3′,5,5′-tetrahydroxy-4′-methoxystilbene.[5] The manner of attachment of the two $C_{15}$ units to the central stilbenic moiety could be unambiguously derived from the long-range correlations between the proton signal at δ 5.83 and the carbon resonances at δ 62.3, 104.7, 119.5, 128.2, 128.4, 164.6, 175.8 and between the proton signal at δ 5.86 and the carbon resonances at δ 62.1, 104.7, 118.2, 128.2, 128.4, 164.6, 175.9. The above evidence allowed us to deduce for gloriosaol A, a spirostructure including two γ-lactone rings, containing the same basic $C_{15}$ and $C_{14}$ structural units of yuccaols C–E but differing

**Table 1**. $^{13}C$ and $^{1}H$ NMR data of gloriosaol A (**1**)[a]

| | Gloriosaol A (**1**) | | | |
|---|---|---|---|---|
| | $\delta_C$ | $\delta_H$ ($J$, Hz) | $\delta_C$ | $\delta_H$ ($J$, Hz) |
| Ring H | | | Ring C | |
| 2 | 93.7 | 5.83 | 93.4 | 5.86 |
| 3 | 62.3 | — | 62.1 | — |
| 4 | 175.8 | — | 175.9 | — |
| Ring F | | | Ring A | |
| 5 | 156.6 | — | 156.6 | — |
| 6 | 97.1 | 5.98 (1.8) | 97.1 | 5.96 (1.8) |
| 7 | 162.4 | — | 162.4 | — |
| 8 | 90.7 | 6.17 (1.8) | 90.7 | 6.16 (1.8) |
| 9 | 164.6 | — | 164.6 | — |
| 10 | 104.7 | — | 104.7 | — |
| Ring G | | | Ring B | |
| 1′ | 128.4 | — | 128.4 | — |
| 2′ | 128.2 | 6.91 (8.5) | 128.2 | 6.90 (8.5) |
| 3′ | 115.7 | 6.71 (8.5) | 115.7 | 6.73 (8.5) |
| 4′ | 159.2 | — | 159.2 | — |
| 5′ | 115.7 | 6.71 (8.5) | 115.7 | 6.73 (8.5) |
| 6′ | 128.2 | 6.91 (8.5) | 128.2 | 6.90 (8.5) |
| Ring E | | | Ring D | |
| 1′ | 130.2 | — | 137.0 | — |
| 2′ | 119.5 | — | 118.2 | — |
| 3′ | 145.9 | — | 155.6 | — |
| 4′ | 133.5 | — | 98.5 | 6.41 (1.8) |
| 5′ | 151.7 | — | 160.3 | — |
| 6′ | 109.1 | 6.57 | 108.3 | 6.47 (1.8) |
| α | 126.8 | 7.06 (16.1) | | |
| β | 125.9 | 7.00 (16.1) | | |
| OMe | 60.9 | 3.84 | | |

[a] Assignments were obtained by 2D-COSY, HSQC, and HMBC data analyses.

**Table 2**. $^{13}C$ and $^{1}H$ NMR data of gloriosaol B (**2**)[a]

| | Gloriosaol B (**2**) | | | |
|---|---|---|---|---|
| | $\delta_C$ | $\delta_H$ ($J$, Hz) | $\delta_C$ | $\delta_H$ ($J$, Hz) |
| Ring H | | | Ring C | |
| 2 | 93.4 | 5.87 | 93.4 | 5.86 |
| 3 | 61.9 | — | 62.1 | — |
| 4 | 175.5 | — | 175.9 | — |
| Ring F | | | Ring A | |
| 5 | 156.0 | — | 156.0 | — |
| 6 | 97.5 | 5.91 (1.8) | 97.5 | 5.92 (1.8) |
| 7 | 162.0 | — | 162.0 | — |
| 8 | 90.6 | 6.17 (1.8) | 90.6 | 6.16 (1.8) |
| 9 | 164.6 | — | 164.6 | — |
| 10 | 104.4 | — | 104.4 | — |
| Ring G | | | Ring B | |
| 1′ | 127.7 | — | 128.3 | — |
| 2′ | 127.0 | 6.91 (8.5) | 128.0 | 6.90 (8.5) |
| 3′ | 115.8 | 6.71 (8.5) | 115.8 | 6.73 (8.5) |
| 4′ | 159.2 | — | 159.2 | — |
| 5′ | 115.8 | 6.71 (8.5) | 115.8 | 6.73 (8.5) |
| 6′ | 127.0 | 6.91 (8.5) | 128.0 | 6.90 (8.5) |
| Ring E | | | Ring D | |
| 1′ | 130.0 | — | 136.4 | — |
| 2′ | 119.5 | — | 118.1 | — |
| 3′ | 145.7 | — | 155.7 | — |
| 4′ | 133.2 | — | 98.4 | 6.41 (1.8) |
| 5′ | 151.6 | — | 159.9 | — |
| 6′ | 109.0 | 6.69 | 108.0 | 6.60 (1.8) |
| α | 127.0 | 7.08 (16.1) | | |
| β | 125.7 | 7.02 (16.1) | | |
| OMe | 60.9 | 3.84 | | |

[a] Assignments were obtained by 2D-COSY, HSQC, and HMBC data analyses.

from yuccaols C–E for the occurrence of two $C_{15}$ units instead of one.[5,7] Taking into account their probable flavonoid origin, the $C_{15}$ units have been numbered as a flavonoid skeleton, as in the case of yuccaols.[7] Thus, the first $C_{15}$ unit consists of rings A, B, C, the central stilbenic moiety of rings D and E, and the latter $C_{15}$ unit is made up of rings F, G, and H. The ROESY experiment of gloriosaol A showed ROE effects between H-2 of ring H and H-α, H-β, and between H-2 of ring C and H-α, H-β. As previously reported, inspection of molecular models and computer representations suggested that these effects were expected for the isomers having H-2 of the $C_{15}$ unit at the same side of the stilbenic moiety and the *p*-hydroxyphenyl ring of the $C_{15}$ unit at the opposite side.

$^{1}H$ and $^{13}C$ NMR data of gloriosaol B (Table 2) were almost superimposable on those of gloriosaol A, some minor differences could be observed for the chemical shifts of H-6′ of ring E ($\delta$ 6.69 in gloriosaol A vs 6.57 in gloriosaol B) and H-6 of ring D ($\delta$ 6.60 in gloriosaol A vs 6.47 in gloriosaol B). Inspection of the ROESY spectrum also revealed in this case ROE effects in agreement with the configuration showing H-2 of the $C_{15}$ unit at the same side of the stilbenic moiety. In both compounds gloriosaol A and gloriosaol B, the protons showing the largest difference in the $^{1}H$ chemical shifts, $H\text{-}6_{ring\ D}$ and $H\text{-}6'_{ring\ E}$, did not exhibit any crucial cross peak in the ROESY that is necessary to determine different structural features.

These considerations suggested to us two hypotheses: (1) the two compounds could be atropisomers of **1**, which is the compound suggested by biogenetic considerations. Such a phenomenon could be caused by a restriction of the free rotation around the double bond due to a steric congestion of the bulky phenolic portions; (2) the two compounds could be two configurational isomers, indicating, in this case, a nonstereoselective biogenetic formation of the stereogenic center C-2.

## 2.2. Determination of the relative configuration of gloriosaols A and B

In order to investigate the former hypothesis, we applied a combined strategy based on the determination of possible chemical exchange phenomena through NMR and on the quantum mechanical calculation of the potential energy surface of **1** obtained upon variation of the involved dihedral angles. Firstly, the analysis of the calculated potential energy surfaces obtained considering all the combinations of the two dihedral angles including the atoms ($\varphi$, $C_{2D}C_{1D}C_{\alpha}C_{\beta}$ and $\psi$, $C_{2'E}C_{1'E}C_{\beta}C_{\alpha}$) was carried out for compound **1**. In particular, the conformational search performed at empirical (MMFFs force-field) and semi-empirical (PM3) levels on compound **1** model structure upon a systematic variation of 5° steps of two dihedral angles provided a series of minimum energy conformers that were separated by small energy barriers (ca. 4.2–4.8 kcal/mol), while the calculated rotational barrier was around 6 kcal/mol. Together with this observation, we also found that compound **2**, the diastereoisomer built upon inversion of configurations at C-2 and C-3 of ring C, submitted to the analogous conformational search, was characterized by minimum energy conformations with small energy discrepancies. In Figure 1 the

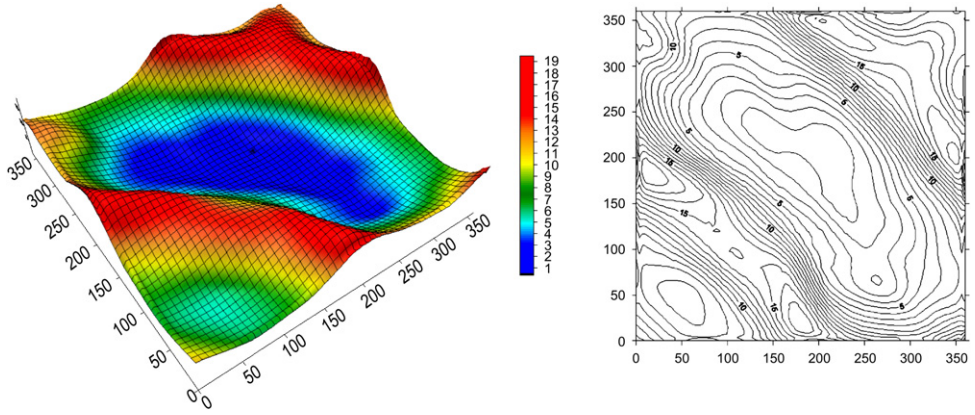

**Figure 1**. Three-dimensional surface (left) and contour plot (right) representation of the potential energy values (kcal/mol) of gloriosaol A (**1**) versus $\varphi$ ($C_{2D}C_{1D}C_{\alpha}C_{\beta}$) and $\psi$ ($C_{2'E}C_{1'E}C_{\beta}C_{\alpha}$) dihedral angles (°).

three-dimensional potential energy surface and the contour plot derived from the same data as a function of $\varphi$ and $\psi$ dihedral angles for compound **1** are reported.

Following the exclusion of the atropisomerism phenomenon for gloriosaols A and B, we aimed to demonstrate that the two compounds were diastereoisomers corresponding to

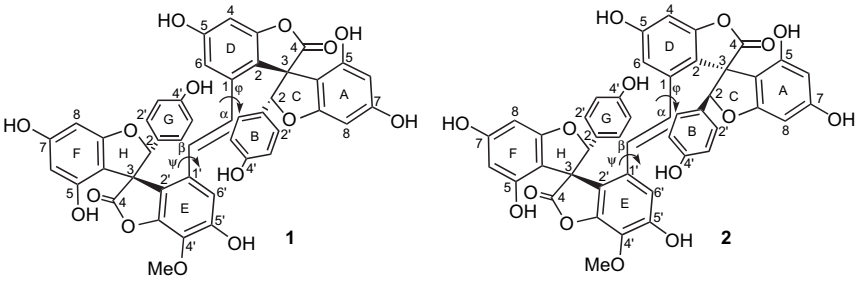

Moreover, we executed on each gloriosaol, dissolved in DMSO-$d_6$, the $^1$H mono-dimensional spectra at various temperatures focusing on H-6$_{\text{ring D}}$ and H-6′$_{\text{ring E}}$. As can be clearly observed in the two sets of $^1$H NMR spectra of gloriosaol A (Fig. 2), resonances H-6$_{\text{ring D}}$ and H-6′$_{\text{ring E}}$ showed no significant changes in their chemical shifts over a wide range of temperatures (300–413 K), a finding in contrast with the conformational interconversion hypothesis and with the low energy barriers suggested by our previous potential energy surfaces analysis. Finally, we mixed both gloriosaols A and B and a series of $^1$H mono-dimensional spectra recorded over the temperatures 300–413 K still indicated two sets of signals.

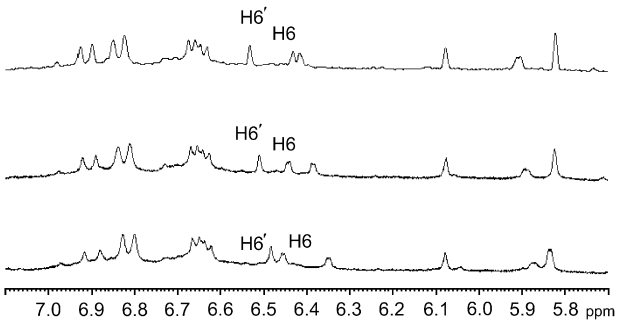


**Figure 2**. Expanded region of $^1$H mono-dimensional spectra of gloriosaol A at 300 (bottom), 345 (middle), and 393 K (top).

the structures **1** and **2**. For this purpose, we chose to further optimize the geometries of the minimum energy conformations for the diastereoisomers **1** and **2**, at MPW91PW91 level,[24] using the 6-31G-(d) basis set, and, in order to obtain an accurate prediction of the chemical shifts, single point GIAO calculations[25] using the same functional and the 6-31G-(d,p) basis set provided us with the $^1$H theoretical values.[26] Moreover, due to the high structural similarity of the two compounds, and therefore to the intrinsically small differences between most of the corresponding resonances, our investigation of the $^1$H chemical shift values was carried out taking into consideration, singularly, the $^1$H calculated values for H-6$_{\text{ring D}}$ and H-6′$_{\text{ring E}}$, which were the only resonances that exhibit significant variations in the chemical shifts of gloriosaols A and B (see Supplementary data). The comparative analysis of the calculated and experimental values, based on the $|\Delta\delta|$ values reported in Table 3, allowed us to unambiguously assign the relative configuration of gloriosaols A and B. In fact, the chemical shift calculated values for H-6$_{\text{ring D}}$ and H-6′$_{\text{ring E}}$ of **1** were in good agreement with the corresponding experimental values observed for gloriosaol A ($|\Delta\delta|$ of 0.04 and 0.04 ppm), while the results obtained for diastereoisomer **2** exhibited deviations of 0.13 and 0.09 ppm with respect to the experimental data of gloriosaol A. Moreover, the experimental c.s. values of H-6$_{\text{ring D}}$ and H-6′$_{\text{ring E}}$ of gloriosaol B were nicely reproduced by theoretical data of **2** ($\Delta\delta$ of 0.00 and 0.03 ppm) while more significant differences were displayed by the calculated data

**Table 3**. Experimental values of H-$6_{ring\ D}$ and H-$6'_{ring\ E}$ for gloriosaol A and gloriosaol B and calculated values of H-$6_{ring\ D}$ and H-$6'_{ring\ E}$ for **1** and **2** ($\delta$, ppm). Comparison, expressed as $\Delta\delta$ values, between experimental and calculated c.s. values

| Atom | Gloriosaol A | **1** | **2** | $\lvert\Delta\delta\rvert$ Gloriosaol A−**1** | $\lvert\Delta\delta\rvert$ Gloriosaol A−**2** |
|---|---|---|---|---|---|
| H-6 (ring D) | 6.47 | 6.43 | 6.60 | 0.04 | 0.13 |
| H-6′ (ring E) | 6.57 | 6.53 | 6.66 | 0.04 | 0.09 |
| Atom | Gloriosaol B | **1** | **2** | $\lvert\Delta\delta\rvert$ Gloriosaol B−**1** | $\lvert\Delta\delta\rvert$ Gloriosaol B−**2** |
| H-6 (ring D) | 6.60 | 6.43 | 6.60 | 0.17 | 0.00 |
| H-6′ (ring E) | 6.69 | 6.53 | 6.66 | 0.16 | 0.03 |

$|\Delta\delta| = |\delta_{exp} - \delta_{calcd}|$, differences for experimental versus mean calculated $^1$H NMR c.s. in absolute value.

of **1** ($\Delta\delta$ of 0.17 and 0.16 ppm). The above evidence allowed us to attribute the structure **1** to gloriosaol A and the structure **2** to gloriosaol B.

The variations for H-$6_{ring\ D}$ and H-$6'_{ring\ E}$ may arise from the different positioning of H-6 and H-6′ in gloriosaol A (**1**) and gloriosaol B (**2**) (Fig. 3). In fact, in the three-dimensional structure of **2**, H-6 and H-6′ are directed toward rings F and A, respectively, probably exerting CH/$\pi$ interactions. On the other hand, the corresponding H-6 and H-6′ in **1** do not point to rings F and A and are, for this reason, in a different chemical and magnetic environments.

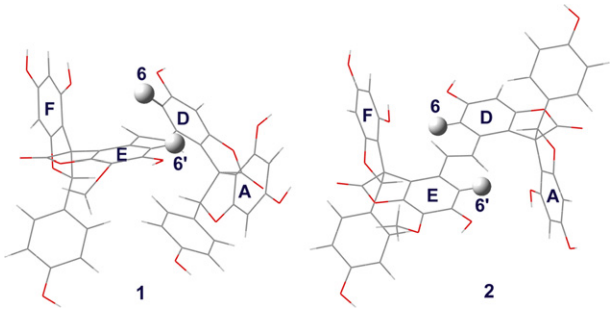


**Figure 3**. Differences in the spatial arrangements of H-$6_{ring\ D}$ and H-$6'_{ring\ E}$ of structures **1** and **2**.

A final corroboration of our configurational assignment has been obtained by the analysis of the ROE cross peaks on the basis of distances measured through a careful examination of the calculated structures of the two diastereoisomers. In particular, the distances of 3.31 and 4.50 Å between H-$6'_{ring\ E}$ and H-$2_{ring\ C}$ together with the distances of 3.33 and 4.50 Å between H-$6_{ring\ D}$ and H-$2_{ring\ H}$ for the stereoisomers **1** and **2**, respectively, were in accordance with the presence of two expected cross peaks observed in the ROESY spectra of gloriosaol A and the absence in the spectra of gloriosaol B.

## 3. Conclusions

Gloriosaols A (**1**) and B (**2**), two novel phenolic derivatives characterized by unusual spirostructures made up of two $C_{15}$ units linked via a $\gamma$-lactone to a central stilbenic portion, were isolated from the roots of *Y. gloriosa*. Their structures have been extensively characterized by means of a combined NMR-Quantum Mechanical approach. This methodology based on quantum mechanical calculations of the geometries and of the $^1$H chemical shifts and their comparison with the experimental, in combination with the analysis of the ROE data, was successful to demonstrate that gloriosaols A (**1**) and B (**2**) are diastereoisomeric compounds and led us to assess the relative configuration of the two diastereomers, indicating a nonstereoselective biogenetic formation of the stereogenic center C-2.

## 4. Experimental

### 4.1. General

Optical rotations were measured on a Jasco DIP 1000 polarimeter. UV spectra were recorded on a UV-2101PC Shimadzu UV–vis Scanning spectrophotometer. IR measurements were obtained on a Bruker IFS-48 spectrometer. Exact masses were measured by a Q-Star Pulsar (Applied Biosystems, 850 Lincoln Centre Drive, Foster City, CA, USA) triple-quadrupole orthogonal time-of-flight (TOF) instrument. Electrospray ionization was used in TOF mode at 8.500 resolving power. Samples were dissolved in pure methanol, mixed with the internal calibrant, and introduced directly into the ion source by direct infusion. Calibration was performed on the peaks of cesium iodide and synthetic peptide (TOF positive ion calibration solution, Bachem, Bachem Distribution Services GmbH, Weil am Rhein, Germany) at *m/z* 132.9054 and 829.5398, respectively. Ions were detected in the mass range of 100–1000 atomic mass units. ESI-MS analyses were performed using a ThermoFinnigan (San Josè, CA, USA) LCQ Deca XP Max ion trap mass spectrometer equipped with Xcalibur software. Samples were dissolved in methanol and infused into the ES ionization source using a syringe pump at a flow rate of 3 μl/min. The capillary voltage was at 40 V, the spray voltage was at 4.8 kV, and the tube lens offset was at 35 V. The capillary temperature was 220 °C. Data were acquired in $MS^1$ and $MS^n$ scanning mode operating in positive ion mode. NMR experiments were performed on a Bruker DRX-600 spectrometer at 300 K. All spectra were acquired in the phase-sensitive mode and the TPPI method was used for quadrature detection in the $\omega_1$ dimension. NMR samples were prepared by dissolving gloriasols A (3.6 mg) and B (1.7 mg) in $CD_3OD$ (Sigma–Aldrich, 99.96% D). The spectra were calibrated using the solvent signal as internal standard ($^1$H, $\delta$=3.34 ppm; $^{13}$C, $\delta$=49.0 ppm).

For gloriosaol A, a total of 32 scans/$t_1$ value were acquired for the HSQC[27] spectrum (4.6 ms), while the HMBC[28] spectrum was executed by recording a total of 96 scans/$t_1$ with a $t_{1max}$ of 3.7 ms. For gloriosaol B, a total of 64 scans/$t_1$ value were acquired for the HSQC spectrum (3.1 ms), while the HMBC spectrum was executed by recording a total of 512 scans/$t_1$ with a $t_{1max}$ of 2.5 ms.

For both gloriosaols A and B, the ROESY[29] spectra were executed with a number of 16 scans/$t_1$, a $t_{1max}$ value of 53.3 ms, and a mixing time of 400 and 600 ms. The NMR data were processed on a Silicon Graphic Indigo2 Workstation using UXNMR software.

$^1$H mono-dimensional spectra were performed on Bruker Avance-300 at various temperatures dissolving both the samples in DMSO-$d_6$ (Carlo Erba, 99.96%).

Column chromatography was performed over Sephadex LH-20 (Pharmacia) and HPLC separations were carried out on an HP 1100 system (Agilent, Palo Alto, CA, USA) equipped with a Waters μ-Bondapack semi-preparative $C_{18}$ column. TLC was performed on silica gel $F_{254}$ (Merck) plates, and reagent grade chemicals (Carlo Erba) were used throughout.

### 4.2. Computational details

In order to allow a full exploration of the conformational space, MM/MD calculations on each of the gloriosaols were performed on Pentium-4 at 2.8 GHz processor using the MMFFs force-field and the MonteCarlo Multiple Minimum (MCMM) method of the MacroModel package. All the structures so obtained (ca. 1000) were minimized using the Polak-Ribier Conjugate Gradient algorithm (PRCG, maximum derivative less than 0.05 kcal/mol). This led to the selection of the lowest energy minimum conformer for each gloriosaol. A subsequent conformational search was carried out first at empirical (MMFFs force-field) and then at semi-empirical (PM3) level on the above selected model structures upon a systematic variation of 5° steps of two dihedral angles $\varphi$ ($C_{2D}C_{1D}C_{\alpha}C_{\beta}$) and $\psi$ ($C_{2'E}C_{1'E}C_{\beta}C_{\alpha}$), allowing to obtain the related potential energy surfaces. The initial geometries of the minimum energy conformers taken from the energy surfaces for gloriosaols A and B were optimized at the hybrid DFT MPW91PW91 level using the 6-31G(d) basis set (Gaussian 03 Software Package).[30] GIAO $^1$H calculations were performed using the mPW1PW91 functional and the 6-31G(d,p) basis set, using as input the geometry previously optimized at mPW1PW91/6-31G(d) level.

### 4.3. Plant material

The roots of *Y. gloriosa* were collected in December 2003 in the experimental field of the Institute of Pharmacochemistry of the Academy of Sciences, Tbilisi, Georgia. A voucher specimen (no. 259) was deposited at the Institute of Pharmacochemistry.

### 4.4. Extraction and isolation

The powdered roots (100 g) were extracted with 80% MeOH yielding 14 g of extract, which was partitioned between water and ethyl acetate yielding 10 g of ethyl acetate extract. Part of this extract (2 g) was fractionated on Sephadex LH-20 (100×5 cm) using MeOH as mobile phase, and 150 fractions (8 mL) were obtained. Fractions 81–120 (115 mg) were chromatographed by RP-HPLC on a Waters μ-Bondapack semi-preparative $C_{18}$ column (300×7.8 mm i.d.) using $CH_3CN$–$H_2O$ (35:65) acidified with 0.05% trifluoroacetic acid as mobile phase (flow rate 2.5 mL/min) to yield compounds **2** (2.5 mg, $t_R$ 27.5) and **1** (3.72 mg, $t_R$ 43.6).

**4.4.1. Gloriosaol A (1).** Brown amorphous powder; $[\alpha]_D^{24}$ +60.1 (*c* 0.2, MeOH); UV (MeOH) $\lambda_{max}$ (log $\varepsilon$): 320 (3.87), 230 (4.36); IR (KBr) $\nu_{max}$ 2918, 1791, 1623, 1509, 1455, 1397, 1202, 1132, 1074, 1020 cm$^{-1}$; for $^1$H and $^{13}$C NMR data, see Table 1; ESI-MS *m/z* 811 $[M+H]^+$, 833 $[M+Na]^+$; ESI-MS/MS *m/z* 717 $[M+H-94]^+$, 419 $[M+H-392]^+$, 269 $[M+H-542]^+$; HRMS (MALDI) $[M+H]^+$ found: 811.1688, $C_{45}H_{31}O_{15}$ requires: 811.1662.

**4.4.2. Gloriosaol B (2).** Brown amorphous powder; $[\alpha]_D^{24}$ +12.8 (*c* 0.2, MeOH); UV (MeOH) $\lambda_{max}$ (log $\varepsilon$): 322 (3.85), 230 (4.30); IR (KBr) $\nu_{max}$ 2918, 1791, 1623, 1509, 1455, 1397, 1202, 1132, 1074, 1020 cm$^{-1}$; for $^1$H and $^{13}$C NMR data, see Table 2; ESI-MS *m/z* 811 $[M+H]^+$, 833 $[M+Na]^+$; ESI-MS/MS *m/z* 717 $[M+H-94]^+$, 419 $[M+H-392]^+$, 269 $[M+H-542]^+$; HRMS (MALDI) $[M+H]^+$ found: 811.1685, $C_{45}H_{31}O_{15}$ requires: 811.1662.

## Supplementary data

Supplementary data associated with this article can be found in the online version, at doi:10.1016/j.tet.2006.10.034.

## References and notes


1. Kemertelidze, E. P.; Pkheidze, T. A. *Khim.-Farm. Zh.* **1972**, *6*, 44–47.
2. Nakano, K.; Yamasaki, T.; Imamura, Y.; Murakami, K.; Takaishi, Y.; Tomimatsu, T. *Phytochemistry* **1989**, *28*, 1215–1217.
3. Nakano, K.; Hara, Y.; Yamasaki, T.; Murakami, K.; Takaishi, Y.; Tomimatsu, T. *Phytochemistry* **1991**, *30*, 1993–1995.
4. Kemertelidze, E.; Benidze, M. *Bull. Georgian Acad. Sci.* **2001**, *164*, 91–93.
5. Oleszek, W.; Sitek, M.; Stochmal, A.; Piacente, S.; Pizza, C.; Cheeke, P. *J. Agric. Food Chem.* **2001**, *49*, 747–752.
6. Piacente, S.; Bifulco, G.; Pizza, C.; Stochmal, A.; Oleszek, W. *Tetrahedron Lett.* **2002**, *43*, 9133–9136.
7. Piacente, S.; Montoro, P.; Oleszek, W.; Pizza, C. *J. Nat. Prod.* **2004**, *67*, 882–885.
8. Piacente, S.; Pizza, C.; Oleszek, W. *Phytochem. Rev.* **2005**, *4*, 177–190.
9. Calderon, A. A.; Zapata, J. M.; Munoz, R.; Pedreno, M. A.; Ros Barcelo, A. *New Phytol.* **1993**, *124*, 455–463.
10. Jeandet, P. R.; Bessis, M.; Sbaghi, M.; Meunier, P. *J. Phytopathol.* **1995**, *143*, 135–139.
11. Langcake, P.; Price, R. J. *Physiol. Plant Pathol.* **1976**, *9*, 77–86.
12. Kimura, Y.; Okuda, H.; Kubo, M. *J. Ethnopharmacol.* **1995**, *45*, 131–139.
13. Orsini, F.; Pellizzoni, F.; Verotta, L.; Aburjai, T.; Rogers, C. B. *J. Nat. Prod.* **1997**, *60*, 1082–1087.
14. Orallo, F. *Curr. Med. Chem.* **2006**, *13*, 87–98.
15. Tsai, S. H.; Lin Shiau, S. H.; Lin, J. K. *Br. J. Pharmacol.* **1999**, *126*, 673–680.
16. Bhat, K. P.; Pezzuto, J. M. *Ann. N.Y. Acad. Sci.* **2002**, *957*, 210–229.
17. Pellecchia, M.; Reed, J. C. *Curr. Pharm. Des.* **2004**, *10*, 1387–1398.
18. Ragione, F. D.; Cucciola, V.; Borriello, A.; Pietra, V. D.; Racioppi, L.; Soldati, G.; Manna, C.; Galletti, P.; Zappia, V. *Biochem. Biophys. Res. Commun.* **1998**, *1250*, 53–58.

19. Olas, B.; Wachowicz, B.; Stochmal, A.; Oleszek, W. *Platelets* **2002**, *13*, 167–173.
20. Olas, B.; Wachowicz, B.; Stochmal, A.; Oleszek, W. *Nutrition* **2003**, *19*, 633–640.
21. Marzocco, S.; Piacente, S.; Pizza, C.; Oleszek, W.; Stochmal, A.; Pinto, A.; Sorrentino, R.; Autore, G. *Life Sci.* **2004**, *75*, 1491–1501.
22. Balestrieri, C.; Felice, F.; Piacente, S.; Pizza, C.; Montoro, P.; Oleszek, W.; Visciano, V.; Balestrieri, M. L. *Biochem. Pharmacol.* **2006**, *71*, 1479–1487.
23. (a) Barone, G.; Duca, D.; Silvestri, A.; Gomez-Paloma, L.; Riccio, R.; Bifulco, G. *Chem.—Eur. J.* **2002**, *8*, 3240–3245; (b) Bifulco, G.; Bassarello, C.; Riccio, R.; Gomez-Paloma, L. *Org. Lett.* **2004**, *6*, 1025–1028; (c) Plaza, A.; Piacente, S.; Perrone, A.; Hamed, A.; Pizza, C.; Bifulco, G. *Tetrahedron* **2004**, *60*, 12201–12209; (d) Bassarello, C.; Zampella, A.; Monti, M. C.; Gomez-Paloma, L.; D'Auria, M. V.; Riccio, R.; Bifulco, G. *Eur. J. Org. Chem.* **2006**, *3*, 604–609.
24. Adamo, C.; Barone, V. *J. Chem. Phys.* **1998**, *108*, 664–675.
25. Ditchfield, R. *J. Chem. Phys.* **1972**, *56*, 5688–5691; Wolinski, K.; Hinton, J. F.; Pulay, P. *J. Am. Chem. Soc.* **1990**, *112*, 8251–8260.
26. Cimino, P.; Duca, D.; Gomez-Paloma, L.; Riccio, R.; Bifulco, G. *Magn. Reson. Chem.* **2004**, *42*, S26–S33.
27. Norwood, T. J.; Boyd, J.; Heritage, J. E.; Soffe, N.; Campbell, I. D. *J. Magn. Reson.* **1990**, *87*, 488–501.
28. Bax, A.; Summers, M. F. *J. Am. Chem. Soc.* **1986**, *108*, 2093–2094.
29. Bax, A.; Davis, D. G. *J. Magn. Reson.* **1985**, *63*, 207–213.
30. Frisch, M. J.; Trucks, G. W.; Schlegel, H. B.; Scuseria, G. E.; Robb, M. A.; Cheeseman, J. R.; Montgomery, J. A., Jr.; Vreven, T.; Kudin, K. N.; Burant, J. C.; Millam, J. M.; Iyengar, S. S.; Tomasi, J.; Barone, V.; Mennucci, B.; Cossi, M.; Scalmani, G.; Rega, N.; Petersson, G. A.; Nakatsuji, H.; Hada, M.; Ehara, M.; Toyota, K.; Fukuda, R.; Hasegawa, J.; Ishida, M.; Nakajima, T.; Honda, Y.; Kitao, O.; Nakai, H.; Klene, M.; Li, X.; Knox, J. E.; Hratchian, H. P.; Cross, J. B.; Adamo, C.; Jaramillo, J.; Gomperts, R.; Stratmann, R. E.; Yazyev, O.; Austin, A. J.; Cammi, R.; Pomelli, C.; Ochterski, J. W.; Ayala, P. Y.; Morokuma, K.; Voth, G. A.; Salvador, P.; Dannenberg, J. J.; Zakrzewski, V. G.; Dapprich, S.; Daniels, A. D.; Strain, M. C.; Farkas, O.; Malick, D. K.; Rabuck, A. D.; Raghavachari, K.; Foresman, J. B.; Ortiz, J. V.; Cui, Q.; Baboul, A. G.; Clifford, S.; Cioslowski, J.; Stefanov, B. B.; Liu, G.; Liashenko, A.; Piskorz, P.; Komaromi, I.; Martin, R. L.; Fox, D. J.; Keith, T.; Al-Laham, M. A.; Peng, C. Y.; Nanayakkara, A.; Challacombe, M.; Gill, P. M. W.; Johnson, B.; Chen, W.; Wong, M. W.; Gonzalez, C.; Pople, J. A. *Gaussian 03W, revision 6.0*; Gaussian: Pittsburgh, PA, 2003.